Published in final edited form as:
*Neuroimage*. 2014 January 15; 85(0 1): . doi:10.1016/j.neuroimage.2013.01.035.

# Somatosensory evoked changes in cerebral oxygen consumption measured non-invasively in premature neonates

**Nadege Roche-Labarbe**[1,2], **Angela Fenoglio**[3], **Harsha Radakrishnan**[1], **Marcia Kocienski-Filip**[4], **Stefan A. Carp**[1], **Jay Dubb**[1], **David A. Boas**[1], **P. Ellen Grant**[3,4], and **Maria Angela Franceschini**[1]

[1]A.A. Martinos Center for Biomedical Imaging, Massachusetts General Hospital - Harvard Medical School, Charlestown, MA, USA

[2]Laboratoire Psychologie des Actions Langagières et Motrices, Université de Caen Basse-Normandie, FRANCE

[3]Fetal-Neonatal Neuroimaging & Developmental Science Center, Children's Hospital Boston, MA, USA

[4]Newborn Medicine, Brigham and Women's Hospital, Boston, MA, USA

## Abstract

The hemodynamic functional response is used as a reliable marker of neuronal activity in countless studies of brain function and cognition. In newborns and infants, however, conflicting results have appeared in the literature concerning the typical response, and there is little information on brain metabolism and functional activation. Measurement of all hemodynamic components and oxygen metabolism is critical for understanding neurovascular coupling in the developing brain.

To this end, we combined multiple near infrared spectroscopy techniques to measure oxy- and deoxy-hemoglobin concentrations, cerebral blood volume (CBV), and relative cerebral blood flow (CBF) in the somatosensory cortex of 6 preterm neonates during passive tactile stimulation of the hand. By combining these measures we estimated relative changes in the cerebral metabolic rate of oxygen consumption ($rCMRO_2$).

CBF starts increasing immediately after stimulus onset, and returns to baseline before blood volume. This is consistent with the model of pre-capillary arteriole active dilation driving the CBF response, with a subsequent CBV increase influenced by capillaries and veins dilating passively to accommodate the extra blood. $rCMRO_2$ estimated using the steady-state formulation shows a biphasic pattern: an increase immediately after stimulus onset, followed by a post-stimulus undershoot due to blood flow returning faster to baseline than oxygenation. However, assuming a longer mean transit time from the arterial to the venous compartment, due to the immature vascular system of premature infants, reduces the post-stimulus undershoot and increases the flow/consumption ratio to values closer to adult values reported in the literature.



Corresponding author: Nadege ROCHE-LABARBE, Lab. PALM - MRSH - SH018, Université de Caen, Campus 1, Esplanade de la Paix, 14000 CAEN, FRANCE, nadege.roche@unicaen.fr, tel: (+33)(0)231 566 216.



The authors have no conflict of interest to disclose.

We are the first to report changes in local rCBF and $rCMRO_2$ during functional activation in preterm infants. The ability to measure these variables in addition to hemoglobin concentration changes is critical for understanding neurovascular coupling in the developing brain, and for using this coupling as a reliable functional imaging marker in neonates.

### Keywords

Oxygen metabolism; functional activation; premature neonates; somatosensory cortex; near infrared spectroscopy; diffusion correlation spectroscopy

## Introduction

The mature brain's functional response to stimulation involves an increase in oxygen metabolism and an even greater hemodynamic response (Fox and Raichle 1986). This disproportionate increase in blood flow over oxygen consumption leads to an increased blood volume (CBV) and oxygenation ($SO_2$) signal in functional near-infrared spectroscopy (fNIRS) and blood oxygen level-dependent (BOLD) signal in functional magnetic resonance imaging (fMRI). This positive functional response is used as a reliable marker of neuronal activity in countless studies of brain function and cognition. In newborns and infants, however, there is little information about brain metabolism and functional activation, though both may differ from those in adults. Unexplained negative functional responses, as well as positive and biphasic responses, have been reported (see Seghier et al. (2006); Lloyd-Fox et al. (2009); Wolf and Greisen (2009) for a review). This is a major obstacle in fundamental and clinical studies of early brain function and cognition.

In order to clarify the functional response in newborns and infants, it is necessary to measure all hemodynamic components and oxygen metabolism. To this end, we combined multiple NIRS techniques to obtain safe and noninvasive measures of functional changes in blood flow, blood volume, oxygenation, and oxygen metabolism in premature infants. In particular, we used diffuse correlation spectroscopy (DCS) to measure relative cerebral blood flow changes (rCBF) (Boas et al. 1995; Durduran et al. 2004), frequency-domain near-infrared spectroscopy (FDNIRS) to measure baseline hemoglobin concentration and saturation (Franceschini et al. 2007), and continuous-wave near-infrared spectroscopy (CWNIRS) to measure hemoglobin concentration and saturation changes. By combining all of these measures we report the relative change in the cerebral metabolic rate of oxygen ($rCMRO_2$) in the somatosensory cortex of preterm newborns during a tactile stimulus. While baseline regional CBF and $CMRO_2$ have been previously measured in neonates using this method (Durduran et al. 2010; Roche-Labarbe et al. 2010) or other optical methods (Edwards et al. 1988; Elwell et al. 2005; Noone et al. 2003; Patel et al. 1998), we are the first to report functional changes in $CMRO_2$.

We first calculated $CMRO_2$ using the steady-state formulation. This common approach simply combines relative changes in blood flow and oxygenation. We then tested two dynamic models. The first model, proposed by Mayhew et al. (2001) and used in rats by Jones et al. (2001) and Dunn et al. (2005), allows us to assign different fractions of functional changes versus baseline values of HbR and HbT concentrations in the venous compartment with respect to the total volume fractions. This is done to compensate for the fact that the NIRS measurements average the hemoglobin changes over the arterial, capillary, and venous compartments and do not provide a direct measure of the changes in the venous compartment alone. The second model, derived from Buxton et al. (1998) and Hoge et al. (2005), allows us to test the influence of the blood transit time from the arterial to venous compartment on the oxygen extraction fraction. While in the steady-state

formulation transit time is considered equal to zero, it is possible that low blood flow in infants has a non-negligible effect on oxygen extraction from the blood during transit from arteries to veins. Our results provide the first account of oxygen metabolism during brain activity in neonates.

## Methods

### 1.Subjects

Between October 2010 and June 2011 in the neonatal ICU at Brigham and Women's Hospital, we recruited 6 neonates born at 33 or 34 weeks GA (2 females), with no known neurological or cardio-respiratory issues. All had APGAR scores ≥ 8 after 5 minutes, with the exception of subject 5, who scored 5 at 5 minutes but reached 8 after 10 minutes. Subjects were not under respiratory support or medication that would modify their vigilance or brain function. Measurements were performed during post-feeding sleep. Only subject 4 had $SaO_2$ monitoring, which was stable between 97 and 100%. We performed functional measurements within the first 2.5 weeks of life and four infants (subjects 1, 2, 3, and 5) were measured twice in this time period. Data from the first measurement session on subject 3 were discarded due to poor DCS signals. Our Institutional Review Board approved the study and parents provided informed consent.

### 2. Techniques and acquisition protocol

To assess relative changes in $CMRO_2$ we combined three NIRS modalities: frequency-domain near-infrared spectroscopy, continuous-wave near-infrared spectroscopy, and diffusion correlation spectroscopy. In particular, for FDNIRS we used a customized commercial frequency-domain oximeter from ISS, Inc. (Champaign IL, USA, www.iss.com) (Franceschini et al. 2007), for CWNIRS we used a CW6 8×8 system made by TechEn, Inc. (Milford, MA, USA, www.techen.com) (Franceschini et al. 2006; Wilcow et al. 2012), and for DCS we used a custom-built device similar to the system developed by Drs. Arjun Yodh and Turgut Durduran at the University of Pennsylvania (Cheung et al. 2001; Durduran et al. 2004; Li et al. 2005). We have previously used these devices in measurements in infants and technical details are reported in several papers (Franceschini et al. 2007; Grant et al. 2009; Roche-Labarbe et al. 2010; Zimmermann et al. 2012). For the present study, the three devices were contained in a small cart, controlled by the same laptop computer, and operated in sequence (Figure 1).

We could have used FDNIRS to measure relative changes during functional measurements, but the availability in our lab of a CW system with a larger number of channels, higher acquisition rate and better signal-to-noise ratio prompted us to use CWNIRS for the functional measurements.

The FDNIRS measurements were performed at the beginning of the session to obtain baseline optical properties at 6 wavelengths ranging from 660 to 830 nm; from these we fit the hemoglobin absorption spectrum to obtain concentration values (Franceschini et al. 2007). We used a rigid handheld probe with sources and detector fibers arranged in a row and separated by 1, 1.5, 2, and 2.5 cm distances, as described by Roche-Labarbe et al. (2010). These small distances are optimal for premature neonates, whose head is about half the size of a 6 months old infant's with much thinner scalp and skull, as shown by experimental results in layered phantoms and Monte Carlo simulations in 3D segmented MRI of a neonate's head (Franceschini et al. 1998; Dehaes et al. 2011; Fabbri et al. 2004). The FDNIRS probe was kept in place over the left somatosensory cortex (position C3 in the 10–20 system) for sixteen seconds of data acquisition. The measurement was repeated five times, with the probe repositioned to account for local inhomogeneities such as hair and

superficial large vessels and thus to ensure that the measurement was representative of the underlying brain region. Measurements were averaged to obtain absolute baseline values.

The CWNIRS and DCS measurements were performed during functional stimulation to measure evoked changes in hemoglobin oxygenation and blood flow. For the CWNIRS measurements we used three source pairs (two lasers each emitting at 690 and 830 nm) and four APD detectors, all coupled to glass fiber bundles. Data from all sources and detectors was simultaneously acquired at 25 Hz. We arranged the three source fibers in a row in a flexible black rubber probe ($5 \times 3 \times 0.5$ $cm^3$) and the four detectors in an X pattern around the central source, with source-detector distances of 1.5 cm (Figure 1). This distance is adequate for a depth penetration of about 0.8–1 cm, which includes the cerebral cortex in preterm neonates (Dehaes et al. 2011). Besides, peripheric channels show a much smaller response than central channels (located over the region of interest), ensuring that we are not measuring systemic changes (Supplementary Fig. 1). For the DCS we used a long coherence length solid state laser emitting at 785 nm coupled to a multimode silica fiber and 4 photon counting APD detectors coupled to single mode fibers. The intensity autocorrelation function of each detector channel was computed by a digital correlator (Correlator.com, Bridgewater, NJ), and an autocorrelation curve was acquired every second over a delay time range of 200 ns to 0.5 s.

For the DCS, the source fiber was set next to the central CWNIRS source, with the detectors arranged in an X pattern next to the CWNIRS detectors, maintaining the same source-detector distances (Figure 2).

The CWNIRS-DCS probe was then strapped over the same cortical area measured with the FDNIRS probe, with the central source located over the C3 position. Continuous CWNIRS and DCS measurements were performed alternatively in 5 minutes long functional runs. We acquired up to 6 functional runs per session (3 CWNIRS and 3 DCS), during which we stimulated the infant's right hand by gently stroking it with a toothbrush. During each run 10 stimuli, 5 seconds long, were presented pseudo-randomly every 20–30 s. Total examination time was 60 min, while subjects were asleep.

## 3. Data processing

**3.1. Frequency-domain near-infrared spectroscopy—**To analyze the FDNIRS data in a standardized fashion we used an automated data analysis routine, which includes data quality assessment and data rejection based on previously established statistical criteria (Franceschini et al. 2007). We used the amplitude and phase data collected at four distances to determine absorption and scattering coefficients at each wavelength (Fantini et al. 1995). We recovered baseline oxygenated and deoxygenated hemoglobin concentrations (HbO and HbR, respectively) for each infant and each measurement session by fitting the absorption coefficients at all wavelengths with the hemoglobin spectra. Total hemoglobin (HbT=HbO +HbR), hemoglobin oxygenation ($SO_2$=HbO/HbT), and cerebral blood volume (Franceschini et al. 2007) were also derived. For these calculations we used extinction coefficients reported in the literature (Wray et al. 1988), assumed a 75% concentration of water (Wolthuis et al. 2001) and, when not available in the clinical charts, we used standard HGB values for age and gestational age (Mäkelä et al. 2008; Jopling et al. 2009). Uncertainties in the above physiologic parameters have previously been reported (Franceschini et al. 2007).

**3.2. Continuous-wave near-infrared spectroscopy—**CWNIRS data were analyzed using Homer2, a graphical user interface we developed for visualization and analysis of near-infrared spectroscopy data (Huppert, Diamond, et al. 2009) (http://www.nmr.mgh.harvard.edu/PMI/resources/homer2/home.htm). Raw data were band-pass

filtered between 0.016 and 0.6 Hz and PCA-based filtering (80% threshold) was applied to reduce motion artifacts. Residual movement artifacts were rejected using an automated detection algorithm based on standard deviation. Block averages over a period of −5 and +25 sec from stimuli onsets were performed and changes in optical density for each source-detector pair were converted to changes in hemoglobin concentration (ΔHbO, ΔHbR, ΔHbT) using the modified Beer–Lambert relationship (Delpy et al. 1988). The differential pathlength factor (DPF) was calculated using the FDNIRS-measured absorption coefficients and an average of the scattering coefficients across infants (6.1 and 4.7 /cm respectively at 690 and 830 nm). Relative changes in blood oxygenation and volume were derived combining hemoglobin FDNIRS baseline values and CWNIRS functional changes:

$$SO_2(t)=\frac{HbO_{FDNIRS}+\Delta HbO_{CWNIRS}(t)}{HbT_{FDNIRS}+\Delta HbT_{CWNIRS}(t)} \quad (1)$$

$$rSO_2=\frac{SO_2(t)}{SO_2(t_0)} \quad (2)$$

$$HbT(t)=HbT_{FDNIRS}+\Delta HbT_{CWNIRS}(t) \quad (3)$$

$$rCBV=\frac{HbT(t)}{HbT(t_0)} \quad (4)$$

**3.3. Diffusion correlation spectroscopy—**Diffuse correlation spectroscopy offers a measure of tissue perfusion that depends on both the movement of scatterers inside the blood vessels and the tissue optical properties (Boas and Yodh 1997; Cheung et al. 2001). The tissue optical properties at 785 nm were derived from the FDNIRS baseline data, and, as for the DPF, we used the absorption coefficient for each subject and each session and the average scattering coefficient across subjects (5.0 /cm at 785 nm).

DCS intensity auto-correlation curves (over a delay time range of 200 ns ~ 1s) acquired sequentially once per second were fitted to the normalized intensity temporal auto-correlation function to obtain a blood flow index ($BF_i$) (Roche-Labarbe et al. 2010). To estimate relative changes in blood flow we used Homer2 and performed an analysis similar to that used for the CWNIRS data. We applied 0.016-Hz high-pass filter to the $BF_i$ normalized data, removed movement artifacts using the automated algorithms, and block averaged the data over the same −5 to +25 sec time period around the stimuli. Finally the relative changes in cerebral blood flow were calculated as:

$$rCBF=\frac{BF_i(t)}{BF_i(t_0)} \quad (5)$$

**3.4. Cerebral metabolic rate of oxygen consumption calculation—**By combining relative changes in blood flow and oxygenation we estimated the relative cerebral metabolic rate of oxygen as:

$$rCMRO_2=rCBF\times rOEF \quad (6)$$

where OEF is the oxygen extraction fraction:

$$rOEF = \frac{SaO_2(t) - SvO_2(t)}{SaO_2(t_0) - SvO_2(t_0)} = \frac{SaO_2(t) - SO_2(t)}{SaO_2(t_0) - SO_2(t_0)} \quad (7)$$

$$\text{with venous oxygenation } SvO_2 = (SO_2 - a \times SaO_2)/b \quad (8)$$

with $a+b=1$, a and b the arterial and venous contributions constant over time (Watzman et al. 2000), and arterial oxygenation $SaO_2$ = 100%.

In addition to the steady-state formulation above, we calculated $rCMRO_2$ using two additional models.

The first model, proposed by (Mayhew et al. 2001) and used in rats by (Jones et al. 2001; Dunn et al. 2005), allows us to assign different fractions of functional changes versus baseline values of HbR and HbT concentrations in the venous compartment with respect to the total volume fractions:

$$rCMRO_2 = \left(1 + \gamma_r \frac{\Delta HbR}{HbR}\right) \times \left(1 + \gamma_t \frac{\Delta HbT}{HbT}\right)^{-1} \times \left(\frac{\Delta CBF + CBF}{CBF}\right) \quad (9)$$

where $\gamma_r$ and $\gamma_t$ are constants used to assign different weights to the venous compartment:

$$\gamma_r = \frac{\Delta HbR_v / \Delta HbR}{HbR_v / HbR} \quad \text{and } \gamma_t = \frac{\Delta HbT_v / \Delta HbT}{HbT_v / HbT}$$

$\gamma_r$ and $\gamma_t$ may range from 0.5 to 2, with 0.75 to 1.25 being a more plausible physiological range (Jones et al. 2001). Under the assumption $SaO_2$=100%, for $\gamma_r$ and $\gamma_t$ equal to 1, equation (8) reduces to equation (6).

The second model, derived from (Buxton et al. 1998) and (Hoge et al. 2005), allows us to test the influence of the blood transit time from the arterial to venous compartment on the oxygen extraction fraction. Using this model we calculated rOEF as:

$$rOEF = \frac{rHbR}{rCBV} + \frac{\tau}{rCBF}\left(\Delta rHbR - \frac{rHbR}{rCBV} \times \Delta rCBV\right) \quad (10)$$

where $\tau$ is the mean transit time through the venous compartment. For $\tau$=0 and $SaO_2$=100%, equation (10) reduces to equation (6). In adults $\tau$ has been estimated to be 3–4 sec (Ibaraki et al. 2007).

**3.5. Additional calculations—**To perform grand averages, for each subject we selected the channel with the strongest CBF and $SO_2$ responses among the four common DCS and CWNIRS channels.

From grand averages, over the interval 3–10 sec after stimulus onset, we estimated the CBF/$CMRO_2$ coupling ratio n, defined as the ratio of the fractional change in CBF to the fractional change in $CMRO_2$ (Davis et al. 1998; Hoge et al. 1999; Blockey et al. 2012):

$$n = \frac{\%rCBF}{\%rCMRO_2} \quad (11)$$

We also calculated the flow/volume coefficient (Grubb et al. 1974) as:

$$\Phi = \frac{\log(rCBV)}{\log(rCBF)} \quad (12)$$

and used this coefficient to convert measured rCBF into rCBV using Grubb's law (which assumes a constant relationship between rCBF and rCBV), to compare this commonly used estimation with our measured rCBV values.

**3.6. Statistics—**For rHbO, rHbR, rCBV, rCBF, rOEF and $rCMRO_2$ we performed Student's t-test for paired samples between subjects' baseline values (average of $t_{-5}$ to $t_{-1}$) and peak or trough values.

We used MATLAB® (http://www.mathworks.com/products/matlab/) for FDNIRS and DCS data processing, Homer2 (http://www.nmr.mgh.harvard.edu/optics/resources/homer2/home.htm, developed by the Optics Division at the Athinoula A. Martinos Center for Biomedical Imaging) for CWNIRS and functional DCS analysis, and Excel® (http://office.microsoft.com/en-us/excel/) for graphics and statistics.

## Results

FDNIRS measurements in our subjects gave the following baseline values (grand average): HbO=38.3±7.8 μMol, HbR=14.7±2.0 μMol, $SO_2$=71.5±2.9%, CBV=2.3±0.5 ml/100g. These are consistent with previous findings from a larger sample at the same gestational age (Roche-Labarbe et al. 2012).

Functional CWNIRS shows the typical neonatal patterns of hemodynamic responses: positive rHbO response (peak at $t_{10}$, p-value < 0.001) and negative rHbR response (trough at $t_{13}$, p-value < 0.001), but the response is slower compared to adult patterns. rCBV peaks at $t_{10}$, p-value < 0.001 (Figure 3). $rSO_2$ increases and rOEF decreases with a trough at $t_{11}$, p-value < 0.001. Functional DCS shows an increase in rCBF that begins at $t_1$ (peak at $t_9$, p-value < 0.001) and returns to baseline at $t_{14}$, before total hemoglobin concentration (Figure 3).

The flow/volume coefficient during activation ($t_3$–$t_{10}$) is $\varphi$=0.24. The Grubb flow/volume relationship predicts rCBV from rCBF data quite well (Pearson's correlation coefficient *r*=0.83). rCBV predicted from Grubb's relationship is very similar to the rCBV measured during the first phase of the response ($t_0$ to $t_9$), but returns to baseline faster (t-test significant at $t_{13}$: pvalue= 0.049) (Fig. 4).

$rCMRO_2$ calculated using equations (6) and (7) shows a biphasic pattern: it starts increasing at $t_1$, peaks at $t_9$ (p-value < 0.001) - which is also when rCBF peaks - decreases with a trough below baseline at $t_{14}$ (p-value < 0.001), and then returns to baseline (Figure 5). This large undershoot is visible in 6 of 9 individual averages, the other 3 measurements being the noisiest ones.

Using equation (9), increasing both $\gamma_r$ and $\gamma_t$ increases OEF changes, decreases the $rCMRO_2$ peak amplitude, and increases the undershoot amplitude. Decreasing both $\gamma_r$ and $\gamma_t$ has opposite effects. Changing only one of the two parameters has a similar effect to changing both parameters, slightly changing the shape of $rCMRO_2$ and rOEF (Supplementary Fig. 2).

Using equations (6) and (10), increasing transit time causes OEF to increase and $CMRO_2$ to decrease. The $rCMRO_2$ undershoot disappears at longer transit times. When $\tau$ is increased, the post-stimulus undershoot amplitude is reduced more than the peak amplitude so that the relative difference between peak and undershoot increases (Fig.6).

Using $rCMRO_2$ calculated with equations (6) and (7), the flow/consumption ratio during activation ($t_3$–$t_{10}$) is $n$=1.5. Using $rCMRO_2$ calculated with equation (9), $n$=1.7 for $\gamma_r$ and $\gamma_t$=1.25, $n$=1.3 for $\gamma_r$ and $\gamma_t$=0.75, and $n$=1.2 for $\gamma_r$ and $\gamma_t$=0.5. Using $rCMRO_2$ calculated with rOEF of equation (10), $n$=2.0 for $\tau$=3s, $n$=2.8 for $\tau$=5s, and $n$=3.6 for $\tau$=6s.

We performed several additional tests to verify the robustness of the results.

First, we verified that the DCS and CWNIRS relative changes in intensity were comparable. Because DCS and CWNIRS measurements were performed sequentially, not simultaneously, we compared intensity changes measured with DCS at 785 nm with those calculated at the same wavelength using the hemoglobin changes measured with CWNIRS. DCS intensity changes are noisier, as expected, but there is good agreement both in the magnitude of the changes and in the onset and return to baseline (Pearson's correlation coefficient $r$ = 0.86) (Supplementary Fig. 3).

We also tested the effect of DPF on rOEF and $rCMRO_2$ changes. For each infant and measurement session, in addition to using DPF estimated from FDNIRS-measured absorption coefficients and average scattering coefficients, we used DPF estimated from FDNIRS-measured scattering coefficient for each infant, and constant DPF equal to the mean values (4.3 and 3.3) or equal to the mean values ±1. This analysis was performed only on the CWNIRS data, not on the DCS functional data, because changing baseline optical properties, while affecting $BF_i$, does not change rCBF. By using these DPFs we found negligible differences in rOEF and $rCMRO_2$ in all cases except when using mean DPF+1. In this case $rCMRO_2$ decreased significantly in amplitude with respect to the other cases, but latencies did not change.

Finally, we tested the effect of normal variations in $SaO_2$. Using $SaO_2$ = 97% instead of 100% causes a 12% decrease in OEF and a 6% decrease in $CMRO_2$, which is equivalent to increasing $\gamma_r$ and $\gamma_t$ from 1 to 1.1 in equation 9.

## Discussion

We are the first to report functional changes in cerebral blood flow and cerebral oxygen consumption in premature newborns. We report these parameters together with hemoglobin concentration and oxygenation to provide a more complete picture of metabolic and vascular functional changes during stimulation in the developing brain.

### 1. Blood flow

For the first time, the blood flow functional response is measured in premature infants. Blood flow starts increasing immediately after stimulus onset and returns to baseline prior to hemoglobin concentration, oxygenation, and blood volume. For this reason, predicted CBV calculated from CBF Grubb's relationship and measured CBV agree quite well while CBF increases (until $t_9$), after which the predicted CBV returns to baseline much faster than the measured CBV. This post-stimulus temporal lag between CBF and CBV has previously been reported in animals (Mandeville et al. 1998; Mandeville, Marota, Ayata, Moskowitz, et al. 1999; Jones et al. 2001) and is consistent with models of the functional hemodynamic response (Buxton et al. 1998; Mandeville, Marota, Ayata, Zaharchuk, et al. 1999; Zheng et al. 2002). Current theories attribute the lag between post-stimulus CBF and CBV to the different compartments where signals originate. The CBF response is produced by pre-capillary arterioles' active dilation by endothelial muscles, whereas the CBV increase is influenced largely by passive dilation of capillaries and veins. The higher compliance of the veins relative to arterioles could explain the slower return to baseline of CBV with respect to CBF.

We estimated a flow/volume coefficient during activation ($t_3$–$t_{10}$) of $\phi$= 0.24. This value is lower than Grubb's value of 0.38, reported for steady-state during a hypercapnia challenge in monkeys (Grubb et al. 1974), but it is very close to the $\phi$ reported during functional activation in rats (Mandeville et al. 1998; Mandeville, Marota, Ayata, Moskowitz, et al. 1999; Jones et al. 2001; Sheth et al. 2004) and adult humans (Chen and Pike 2009). Jones et al. (2001) points out that close examination of the data from Mandeville, Marota, Ayata, Moskowitz, et al. (1999) reveals that $\phi$ is approximately 0.2 after 6 sec of activation, but reaches 0.36 after 30 sec of stimulation when a steady state is likely reached. Huppert, Jones, et al. (2009) calculated $\phi$= 0.23 during a 2 sec stimulation. In our protocol, the short stimulation period (5 sec) may justify the lower flow/volume coefficient than is found by Grubb in a steady-state regime.

## 2. Oxygen metabolism

For the first time, oxygen utilization during functional activation is measured in premature infants. $rCMRO_2$ shows a biphasic pattern: an increase immediately after stimulus onset, followed by a significant post-stimulus undershoot due to blood flow returning to baseline faster than oxygenation. Although this $rCMRO_2$ post-stimulus undershoot is not predicted by the balloon/windkessel model (Buxton et al. 1998; Mandeville, Marota, Ayata, Zaharchuk, et al. 1999), an undershoot (smaller in amplitude) is visible in experiments in rats using various imaging techniques (Mandeville, Marota, Ayata, Moskowitz, et al. 1999; Ances et al. 2001; Jones et al. 2001; Sheth et al. 2004; Vazquez et al. 2012). Durduran et al. (2004) used NIRS and DCS in adult human subjects during finger-tapping stimulation and also report a small undershoot. In our subjects, however, the post-stimulus undershoot is very large (about 50% of the amplitude of the positive response peak).

We tested whether this post-stimulus undershoot could be due to the assumptions we make in our calculations. Firstly, because we measured $rSO_2$ and rCBF sequentially, not simultaneously, we verified that intensity changes measured with CWNIRS and with DCS during alternate runs did not differ substantially and could not have caused the measured undershoot in $rCMRO_2$.

Secondly, we verified that assumptions in the DPF, which we estimated assuming a constant scattering coefficient across infants, cannot cause the $rCMRO_2$ undershoot. A 20% increase in DPF reduces the $rCMRO_2$ post-stimulus amplitude by only 18%, and reduces the ratio between post-stimulus and peak amplitude to 37%.

Thirdly, we tested whether assigning different weights to the fractional hemoglobin concentration changes in the venous compartments (Jones et al. 2001; Dunn et al. 2005) could reduce the post-stimulus $rCMRO_2$ undershoot. By decreasing $\gamma_r$ or $\gamma_t$ in equation (9), the peak amplitude of $rCMRO_2$ increases and the post-stimulus undershoot amplitude decreases so that for $\gamma_r$ or $\gamma_t$ equal to 0.75 the undershoot amplitude becomes about 1/3 of the peak amplitude. Further decreasing $\gamma_r$ or $\gamma_t$ further reduces the undershoot, but values of $\gamma$<0.75 are outside the plausible physiological range (Mayhew et al. 2001). Indeed, $\gamma$<1 means that fractional functional changes in hemoglobin concentration are smaller in the venous compartment than in the other compartments. This is unlikely because the venous compartment is the most compliant, even more so in premature infants.

Finally we tested whether assuming arterial to vascular transit times larger than 0 sec would reduce the $rCMRO_2$ post-stimulus undershoot. Using equation (10) (Hoge et al. 2005) we found that larger transit times make rOEF more negative and hence reduce $rCMRO_2$ changes. For a transit time of 3 sec - value assumed for adults (Ibaraki et al. 2007) - $rCMRO_2$ peak amplitude decreases by 25% and post-stimulus undershoot amplitude decreases by ~50%, so that the undershoot amplitude becomes about 1/3 of the peak

amplitude. By further increasing the transit time to 6 sec - a reasonable estimate for infants based on our measured CBV value of 2.3 ml/100g and on CBF values of 20–25 ml/100g/min reported in the fMRI literature (Arichi et al. 2012) - the $rCMRO_2$ post-stimulus undershoot is further reduced to 10% of the peak amplitude.

Assuming a larger transit time not only reduces the post-stimulus undershoot but also increases the flow/consumption ratio to values closer to what is reported in the literature. By considering rCBF and $rCMRO_2$ calculated using equations (6) and (7) in the time interval $t_3$–$t_{10}$ we estimated a flow/consumption ratio $n = 1.5$. This value is consistent with optical studies in adults (Huppert, Jones, et al. 2009; Yücel et al. 2012), but lower than values obtained with other imaging techniques (Buxton 2010; Blockey et al. 2012). Using longer transit times, the flow/consumption ratio increases to values closer to that reported in the literature: assuming $\tau$=3 sec we obtain n=2, and assuming $\tau$=6 sec we obtain n=3.6. In contrast, when we use the compartmental model of equation (9), decreasing $\gamma_r$ and $\gamma_t$, (which reduces the undershoot and increases the peak amplitude), n decreases further from reported literature values. For example, for $\gamma_r$ or $\gamma_t$ =0.75, n=1.3.

Based on these results, it seems reasonable to use larger arterial to venous transit times to estimate OEF and $CMRO_2$ functional changes in premature infants. This could be due to immaturity of the vascular and neural systems. During angiogenesis, large vessels initially penetrate radially from the outside of the brain until mid-pregnancy, then they sprout collaterals (arterioles and veins precursors) that connect by anastomosis and form networks during the second half of pregnancy. After birth, capillary beds start forming in place of anastomosis, triggered by increasing neuronal activity due to exogenous stimulation (see Marin-Padilla (2012) for a review of brain microvasculature development). At the gestational age (34 weeks) and postnatal age (1–2 weeks) we studied, capillary beds are not yet formed in the cortex. Because the vessels are still precursors, endothelial muscles are absent or weak, resulting in a higher compliance of their vascular system (Ballabh et al. 2004; Plessis 2009; Harris et al. 2011). This higher compliance, combined with a lower baseline CBF (Altman et al. 1993), justifies a longer mean transit time.

## 3. Hemoglobin concentration

The hemoglobin concentration functional changes we measured in preterm neonates show the typical patterns of response to sensory stimulation: increases in HbO and decreases in HbR. The “preterm” hemoglobin response, however, is slower (longer time to peak) compared with that in adults, similar to what was recently described using fMRI in preterm newborns (Arichi et al. 2012). This can also be explained by the longer arterial to venous transit time and lower baseline CBF.

Deoxygenation associated with stimulation (also called negative BOLD responses in fMRI literature) has been inconsistently described in infants, thus far without a satisfactory explanation (see Seghier et al. (2006); Lloyd-Fox et al. (2009); Wolf and Greisen (2009) for a review). Consistent with Arichi et al. (2012), we did not observe negative responses in premature newborns. These results in infants <3 weeks of age are also consistent with our previous results in which we observed negative responses in infants between 3–8 weeks of age, but positive responses for younger and older infants (Zimmermann et al. 2012).

## 4. Conclusion

We describe, for the first time, changes in local rCBF and $rCMRO_2$ during functional activation in preterm infants. The ability to measure these variables in addition to hemoglobin concentration changes is critical for understanding neurovascular coupling in the developing brain, and for using the coupling as a reliable functional imaging marker in

neonates. Based on our results, we propose that the functional response to sensory stimulation in premature neonates should be considered typically positive (i.e., an activation), and the hemodynamic response function in this population designed specifically to fit the slower dynamics. Models of the neurovascular response should provide a mean transit time parameter adapted to neonates, arguably one of the most important populations for optical methods. Finally, transit time during the functional response decreases during activation (when vessels dilate) and increases during recovery. So far models of the neurovascular response set it as a constant, the mean transit time, but improved dynamic models could set it dependent on CBF for example.

## Supplementary Material

Refer to Web version on PubMed Central for supplementary material.

## Acknowledgments

The authors thank all the families for their participation in this study and the nurses, physicians, and staff in the Neonatal ICU at Brigham and Women's Hospital for their help and support. In particular, we thank Linda J. Van Marter, Robert M. Insoft, Jonathan H. Cronin, Julianne Mazzawi, and Steven A. Ringer. We thank Drs Ivy Lin and Mathieu Dehaes for their support with the data analysis and Gary Boas for revising the manuscript.

This work was supported by NIH grants R01 HD042908, P41-RR14075 and R21-HD058725 and by the Clinical Translational Science Award UL1RR025758 to Harvard University and Brigham and Women's Hospital from the National Center for Research Resources. The content is solely the responsibility of the authors and does not necessarily represent the official views of the National Center for Research Resources or the National Institutes of Health.

## References

Altman DI, Perlman JM, Volpe JJ, Powers WJ, Altman DI. Cerebral oxygen metabolism in newborns. Pediatrics. 1993; 92:99–104. [PubMed: 8516092]

Ances BM, Wilson DF, Greenberg JH, Detre JA. Dynamic Changes in Cerebral Blood Flow, O2 Tension, and Calculated Cerebral Metabolic Rate of O2 During Functional Activation Using Oxygen Phosphorescence Quenching. 2001; 21:511–516.

Arichi T, Fagiolo G, Varela M, Melendez-Calderon A, Allievi A, Merchant N, Tusor N, Counsell SJ, Burdet E, Beckmann CF, David EA. Development of BOLD signal hemodynamic responses in the human brain. NeuroImage. 2012; 63:663–673. [PubMed: 22776460]

Ballabh P, Braun A, Nedergaard M. Anatomic analysis of blood vessels in germinal matrix, cerebral cortex, and white matter in developing infants. Pediatr Res. 2004; 56:117–124. [PubMed: 15128918]

Blockey NP, Griffeth VEM, Simon AB, Buxton RB. A review of calibrated blood oxygenation level-dependent (BOLD) methods for the measurement of task-induced changes in brain oxygen metabolism. NMR in Biomedicine. 2012

Boas DA, Campbell LE, Yodh AG. Scattering and Imaging with Diffusing Temporal Field Correlations. Physical Review Letters. 1995; 75:1855–1858. [PubMed: 10060408]

Boas DA, Yodh AG. Spatially varying dynamical properties of turbid media probed with diffusing temporal light correlation. Journal of the Optical Society of America. 1997; 14:192–215.

Buxton RB. Interpreting oxygenation-based neuroimaging signals: the importance and the challenge of understanding brain oxygen metabolism. Frontiers in neuroenergetics. 2010; 2:1–16. [PubMed: 20162100]

Buxton RB, Wong EC, Frank LR. Dynamics of blood flow and oxygenation changes during brain activation: the balloon model. Reson Med. 1998; 39:855–864.

Chen JJ, Pike GB. BOLD-specific cerebral blood volume and blood flow changes during neuronal activation in humans. NMR Biomed. 2009; 22:1054–1062. [PubMed: 19598180]

Cheung C, Culver JP, Kasushi T, Greenberg JH, Yodh AG. In vivo cerebrovascular measurement combining diffuse near-infrared absorption and correlation spectroscopies. Physics in Medicine and Biology. 2001; 46:2053–2065. [PubMed: 11512610]

Davis TL, Kwong KK, Weisskoff RM, Rosen BR. Calibrated functional MRI: Mapping the dynamics of oxidative metabolism. proc Natl Acad Sci. 1998; 95:1834–1839. [PubMed: 9465103]

Dehaes M, Grant PE, Sliva DD, Roche-Labarbe N, Pienaar R, Boas DA, Franceschini MA, Selb J. Assessment of the frequency-domain multi-distance method to evaluate the brain optical properties: Monte Carlo simulations from neonate to adult. Biomedical optics express. 2011; 2:552–567. [PubMed: 21412461]

Delpy D, Cope M, van der Zee P, Arridge S, Wray S, Wyatt J. Estimation of optical path length through tissue from direct time of flight measurements. Phys Med Biol. 1988; 33:1433–1442. [PubMed: 3237772]

du Plessis A. Cerebral Blood Flow and Metabolism in the Developing Fetus. Clinics in Perinatology. 2009; 36:531–548. [PubMed: 19732612]

Dunn AK, Devor A, Dale AM, Boas DA. Spatial extent of oxygen metabolism and hemodynamic changes during functional activation of the rat somatosensory cortex. NeuroImage. 2005; 27:279–290. [PubMed: 15925522]

Durduran T, Yu G, Burnett MG, Detre JA, Greenberg JH, Wang J, Zhou C, Yodh AG. Diffuse optical measurement of blood flow, blood oxygenation, and metabolism in a human brain during sensorimotor cortex activation. Optics Letters. 2004; 29:1766–1768. [PubMed: 15352363]

Durduran T, Zhou C, Buckley E, Kim M, Yu G, Choe R, Gaynor JW, Spray TL, Durning SM, Mason SE, Montenegro LM, Nicolson SC, Zimmerman RA, Putt ME, Wang J, Greenberg JH, Detre JA, Yogh AG, Licht DJ. Optical measurement of cerebral hemodynamics and oxygen metabolism in neonates with congenital heart defects. J Biomed Opt. 2010; 15(3) 037004.

Edwards AD, Richardson C, Cope M, Wyatt JS, Delpy DT, Reynolds EOR. Cotside measurement of cerebral blood flow in ill infants by near-infrared spectroscopy. The Lancet. 1988; 332(8614):770–771.

Elwell CE, Henty JR, Leung TS, Austin T, Meek JH, Delpy DT, Wyatt JS. Measurement of CMRO2 in neonates undergoing intensive care using near infrared spectroscopy. Advances in Experimental Medicine and Biology. 2005; 566:263–268. [PubMed: 16594161]

Fabbri F, Sassaroli A, Henry ME, Fantini S. Optical measurements of absorption changes in two-layered diffusive media. Physics in Medicine and Biology. 2004; 49:1183–1201. [PubMed: 15128197]

Fantini S, Franceschini M, Maier JS, Walker SA, Barbieri B, Gratton E. Frequency-domain multichannel optical detector for non-invasive tissue spectroscopy and oximetry. Optical engineering. 1995; 34:34–42.

Fox PT, Raichle ME. Focal Physiological Uncoupling of Cerebral Blood Flow and Oxidative Metabolism during Somatosensory Stimulation in Human Subjects. Proc Natl Acad Sci USA. 1986; 83:1140–1144. [PubMed: 3485282]

Franceschini MA, Fantini S, Paunescu A, Maier JS, Gratton E. Influence of a superficial layer in the quantitative spectroscopic study of strongly scattering media. Applied Optics. 1998; 37:7447–7458. [PubMed: 18301579]

Franceschini MA, Joseph DK, Huppert TJ, Diamond SG, Boas DA. Diffuse optical imaging of the whole head. J Biomed Opt. 2006; 11(5) 054007.

Franceschini MA, Thaker S, Themelis G, Krishnamoorthy KK, Bortfeld H, Diamond SG, Boas DA, Arvin K, Grant PE. Assessment of infant brain development with frequency-domain near-infrared spectroscopy. Pediatric Research. 2007; 61:546–551. [PubMed: 17413855]

Grant PE, Roche-Labarbe N, Surova A, Themelis G, Selb J, Warren EK, Krishnamoorthy KS, Boas DA, Franceschini MA. Increased cerebral blood volume and oxygen consumption in neonatal brain injury. Journal of Cerebral Blood Flow & Metabolism. 2009; 29:1704–1713. [PubMed: 19675563]

Grubb RLJ, Raichle ME, Eichling JO, Ter-Pogossian MM. The effects of changes in PaCO2 on cerebral blood volume, blood flow, and vascular mean transit time. Stroke. 1974; 5:630–639. [PubMed: 4472361]

Harris JJ, Reynell C, Attwell D. The physiology of developmental changes in BOLD functional imaging signals. Developmental Cognitive Neuroscience. 2011; 1:199–216. [PubMed: 22436508]

Hoge RD, Atkinson J, Gill B, Crelier GR, Marrett S, Pike GB. Linear coupling between cerebral blood flow and oxygen consumption in activated human cortex. proc Natl Acad Sci. 1999; 96:9403–9408. [PubMed: 10430955]

Hoge RD, Franceschini MA, Covolan RJM, Huppert T, Mandeville JB, Boas DA. Simultaneous recording of task-induced changes in blood oxygenation, volume, and flow using diffuse optical imaging and arterial spin-labeling MRI. NeuroImage. 2005; 25:701–707. [PubMed: 15808971]

Huppert TJ, Diamond SG, Franceschini MA, Boas DA. HomER: a review of time-series analysis methods for near- infrared spectroscopy of the brain. Applied Optics. 2009; 48:D280–D298. [PubMed: 19340120]

Huppert TJ, Jones PB, Devor A, Dunn AK, Teng IC, Dale AM, Boas DA. Sensitivity of neural-hemodynamic coupling to alterations in cerebral blood flow during hypercapnia. Journal of Biomedical Optics. 2009; 14 044038.

Ibaraki M, Ito H, Shimosegawa E, Toyoshima H, Ishigame K, Takahashi K, Kanno I, Miura S. Cerebral vascular mean transit time in healthy humans: a comparative study with PET and dynamic susceptibility contrast-enhanced MRI. Journal of Cerebral Blood Flow & Metabolism. 2007; 27:404–413. [PubMed: 16736045]

Jones M, Berwick J, Johnston D, Mayhew J. Concurrent Optical Imaging Spectroscopy and Laser-Doppler Flowmetry: The Relationship between Blood Flow, Oxygenation, and Volume in Rodent Barrel Cortex. NeuroImage. 2001; 13:1002–1015. [PubMed: 11352606]

Jopling J, Henry E, Wiedmeier SE, Christensen RD. Reference Ranges for Hematocrit and Blood Hemoglobin Concentration During the Neonatal Period: Data From a Multihospital Health Care System. Pediatrics. 2009; 123:e333–e337. [PubMed: 19171584]

Li J, Dietsche G, Iftime D, Skipetrov SE, Maret G, Elbert T, Rockstroh B, Gisler T. Noninvasive detection of functional brain activity with near-infrared diffusing-wave spectroscopy. Journal of Biomedical Optics. 2005; 10 044002.

Lloyd-Fox S, Blasi A, Elwell CE. Illuminating the developing brain: the past, present and future of functional near infrared spectroscopy. Neurosci Biobehav Rev. 2009

Mandeville JB, Marota JJ, Ayata C, Zaharchuk G, Moskowitz MA, Rosen BR, Weisskoff RM. Evidence of a cerebrovascular postarteriole windkessel with delayed compliance. Journal of Cerebral Blood Flow & Metabolism. 1999; 19:679–689. [PubMed: 10366199]

Mandeville JB, Marota JJA, Ayata C, Moskowitz MA, Weisskoff RM, Rosen BR. MRI Measurement of the Temporal Evolution of Relative CMRO2 During Rat Forepaw Stimulation. Magnetic resonance in medicine. 1999; 42:944–951. [PubMed: 10542354]

Mandeville JB, Marota JJA, Kosofsky BE, Keltner JR, Weissleder R, Rosen BR, Weisskoff RM. Dynamic Functional Imaging of Relative Cerebral Blood Volume During Rat Forepaw Stimulation. Magnetic resonance in medicine. 1998; 39:615–624. [PubMed: 9543424]

Marin-Padilla M. The human brain intracerebral microvascular system: development and structure. Frontiers in neuroanatomy. 2012; 6

Mayhew J, Johnston D, Martingale J, Jones M, Berwick J, Zheng Y. Increased Oxygen Consumption Following Activation of Brain: Theoretical Footnotes Using Spectroscopic Data from Barrel Cortex. NeuroImage. 2001; 13:975–987. [PubMed: 11352604]

Mäkelä E, Takala TL, Suominen P, Matomäki J, Salmi TT, Rajamäki A, Lapinleimu H, Lehtonen L, Irjala K, Lähteenmäki PM. Hematological parameters in preterm infants from birth to 16 weeks of age with reference to iron balance. Clin Chem Lab Med. 2008; 46:551–557. [PubMed: 18605935]

Noone MA, Sellwood M, Meek JH, Wyatt JS. Postnatal adaptation of cerebral blood flow using near infrared spectroscopy in extremely preterm infants undergoing high-frequency oscillatory ventilation. Acta Paediatrica. 2003; 92(9):1079–1084. [PubMed: 14599074]

Patel J, Marks K, Roberts I, Azzopardi D, David EA. Measurement of cerebral blood flow in newborn infants using near ifrared spectroscopy with indocyanine green. Pediatric Research. 1998; 43(1): 34–39. [PubMed: 9432110]

Roche-Labarbe N, Carp SA, Surova A, Patel M, Boas DA, Grant PE, Franceschini MA. Noninvasive optical measures of CBV, StO(2), CBF index, and rCMRO(2) in human premature neonates' brains in the first six weeks of life. Hum Brain Mapp. 2010; 31:341–352. [PubMed: 19650140]

Roche-Labarbe N, Fenoglio A, Aggarwal A, Dehaes M, Carp SA, Franceschini MA, Grant PE. Near-infrared spectroscopy assessment of cerebral oxygen metabolism in the developing premature brain. Journal of Cerebral Blood Flow & Metabolism. 2012; 32:481–488. [PubMed: 22027937]

Seghier ML, Lazeyras F, Huppi PS. Functional MRI of the newborn. Seminars in Fetal & Neonatal Medicine. 2006; 11:479–488. [PubMed: 17000141]

Sheth SA, Nemoto M, Guiou M, Walker M, Pouratian N, Toga AW. Linear and Nonlinear Relationships between Neuronal Activity, Oxygen Metabolism, and Hemodynamic Responses. Neuron. 2004; 42:347–355. [PubMed: 15091348]

Vazquez AL, Fukuda M, Kim S-G. Evolution of the dynamic changes in functional cerebral oxidative metabolism from tissue mitochondria to blood oxygen. Journal of Cerebral Blood Flow & Metabolism. 2012; 32:745–758. [PubMed: 22293987]

Watzman HM, Kurth CD, Montenegro LM, Rome J, Steven JM, Nicolson SC. Arterial and venous contributions to near- infrared cerebral oximetry. Anesthesiology. 2000; 93:947–953. [PubMed: 11020744]

Wilcox T, Stubbs J, Hirshkowitz A, Boas DA. Functional activation of the infant cortex during object processing. NeuroImage. 2012; 62(3):1833–1840. [PubMed: 22634218]

Wolf M, Greisen G. Advances in near-infrared spectroscopy to study the brain of the preterm and term neonate. Clin Perinatol. 2009; 36:807–834. [PubMed: 19944837]

Wolthuis R, van Aken M, Fountas K, Robinson JSJ, Bruining HA, Puppels GJ. Determination of water concentration in brain tissue by Raman spectroscopy. Anal Chem. 2001; 73:3915–3920. [PubMed: 11534716]

Wray S, Cope M, Delpy DT, Wyatt JS, Reynolds EOR. Characterization of the near infrared absorption spectra of cytochrome $aa_3$ and haemoglobin for the non-invasive monitoring of cerebral oxygenation. Biochimica et Biophysica Acta - Bioenergetics. 1988; 933:184–192.

Yücel MA, Huppert TJ, Boas DA, Gagnon L. Calibrating the BOLD signal during a motor task using an extended fusion model incorporating DOT, BOLD and ASL data. NeuroImage. 2012; 61:1268–1276. [PubMed: 22546318]

Zheng Y, Martindale J, Johnston D, Jones M, Berwick J, Mayhew J. A Model of the Hemodynamic Response and Oxygen Delivery to Brain. NeuroImage. 2002; 16:617–637. [PubMed: 12169248]

Zimmermann BB, Roche-Labarbe N, Surova A, Boas DA, Wolf M, Grant PE, Franceschini MA. The Confounding Effect of Systemic Physiology on the Hemodynamic Response in Newborns. Adv Exp Med Biol. 2012; 737:103–109. [PubMed: 22259089]

## Highlights

- We know little of brain metabolism during functional activation in neonates
- This is a major obstacle in studies of early brain function and cognition
- We combined three nearinfrared spectroscopy techniques
- We stimulated the somatosensory cortex of premature neonates
- We measured functional changes in the cerebral metabolic rate of oxygen consumption

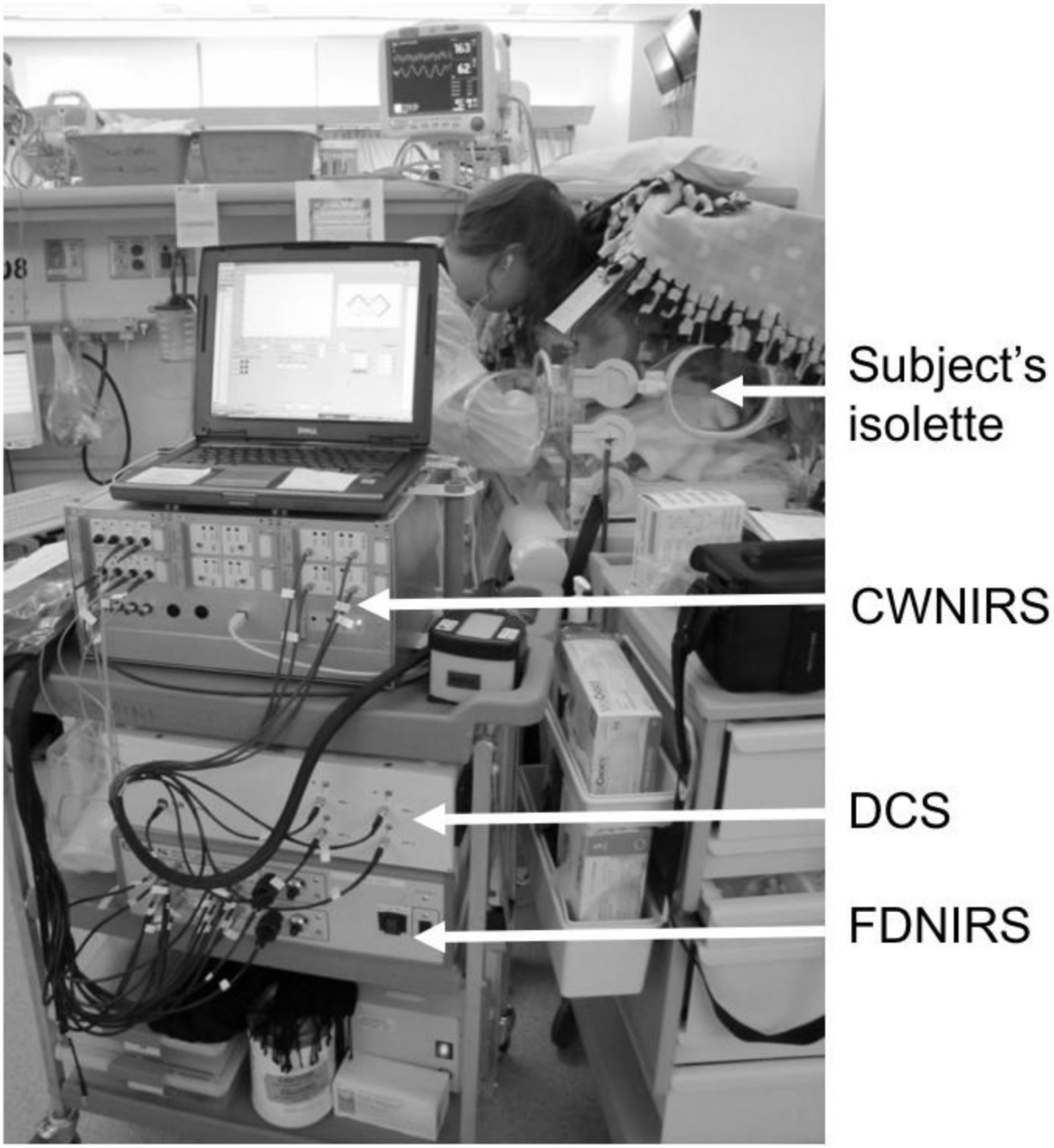


**Fig. 1.**
Experimental set-up.

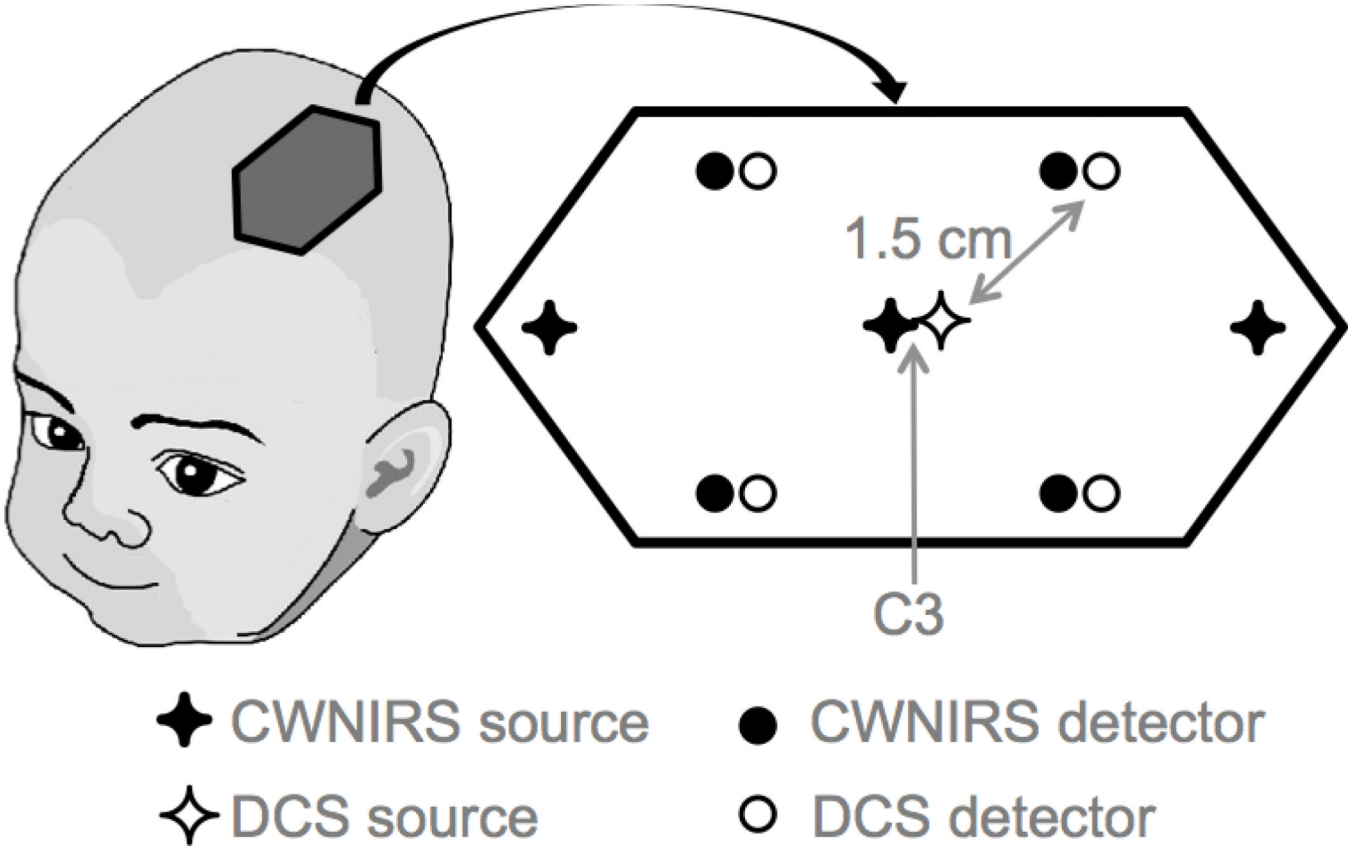


**Fig. 2.**
Schema of the CWNIRS-DCS probe. The probe was secured over the left somatosensory cortex, centered on the C3 position in the 10–20 electrode placement system.

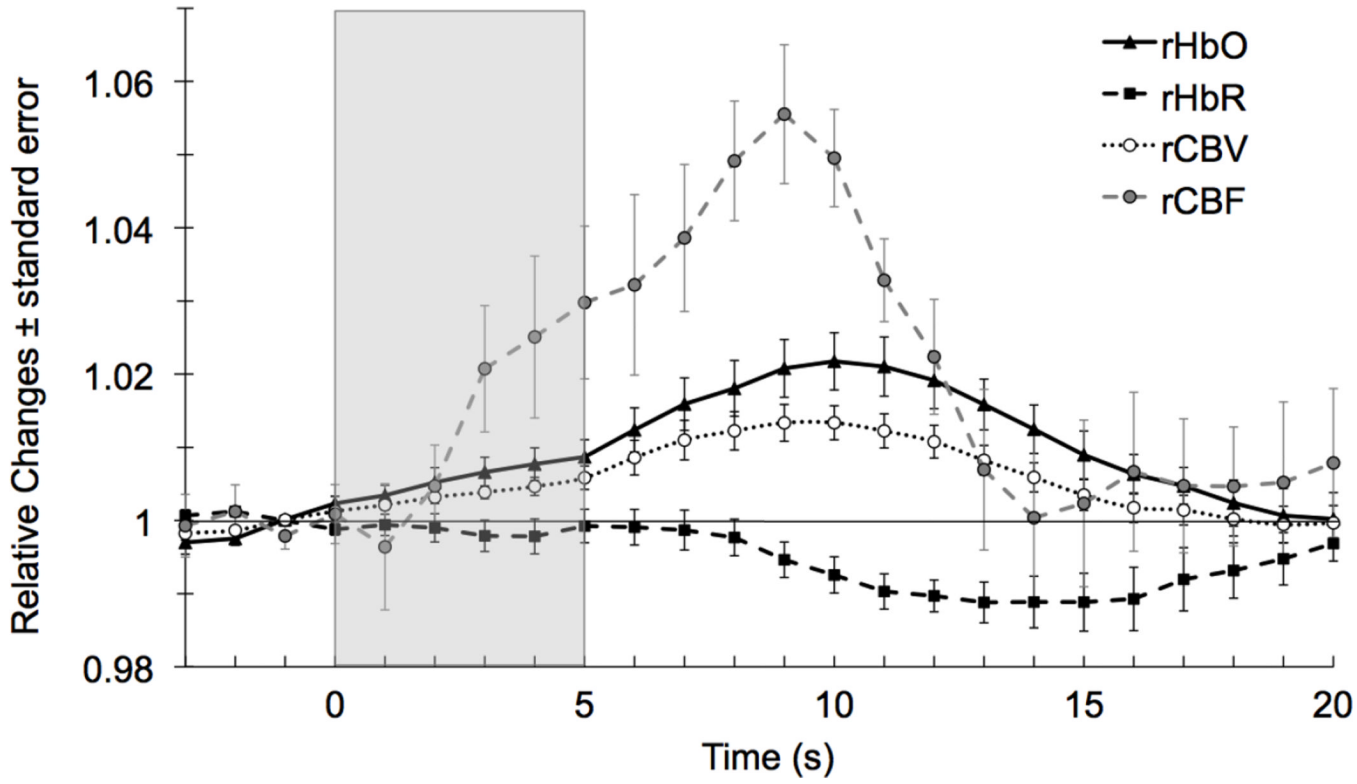


**Fig. 3.**
Grand average of relative changes in blood flow, oxy-, deoxy- and total hemoglobin.

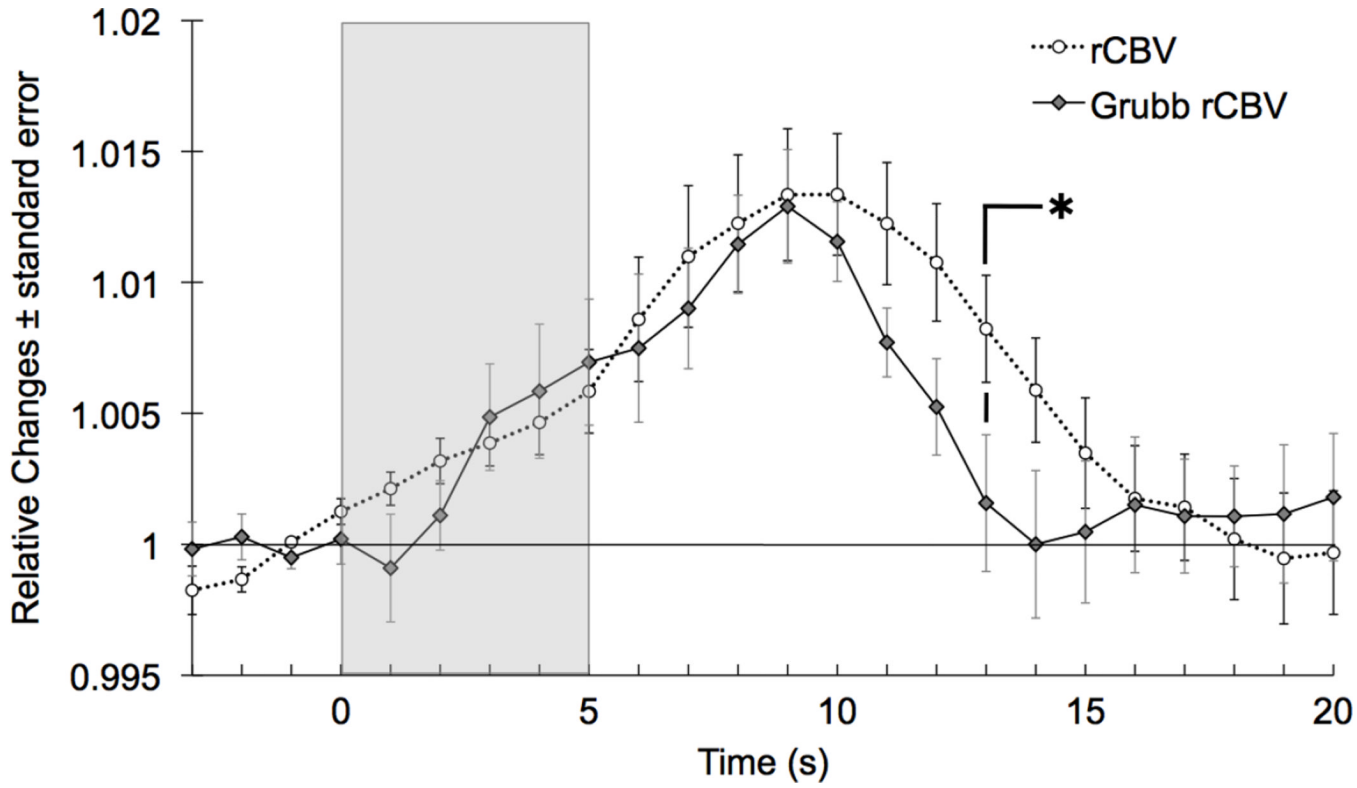


**Fig. 4.**

Grand average of relative changes in cerebral blood volume measured with NIRS and estimated from the DCS blood flow using the Grubb relationship and $\varphi$=0.24. Values are significantly different at $t_{13}$.

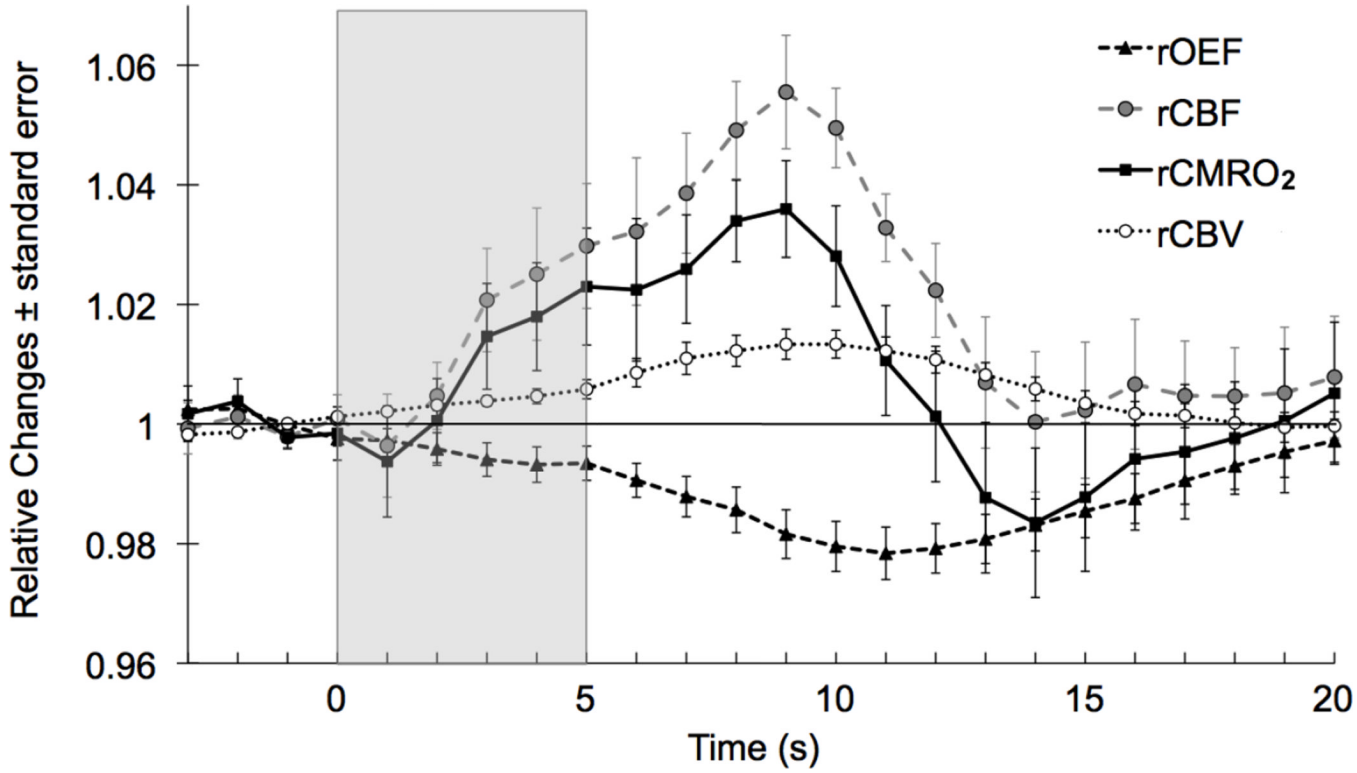


**Fig. 5.**
Grand average of relative changes in oxygen extraction fraction, cerebral blood flow, cerebral metabolic rate of oxygen and cerebral blood volume.

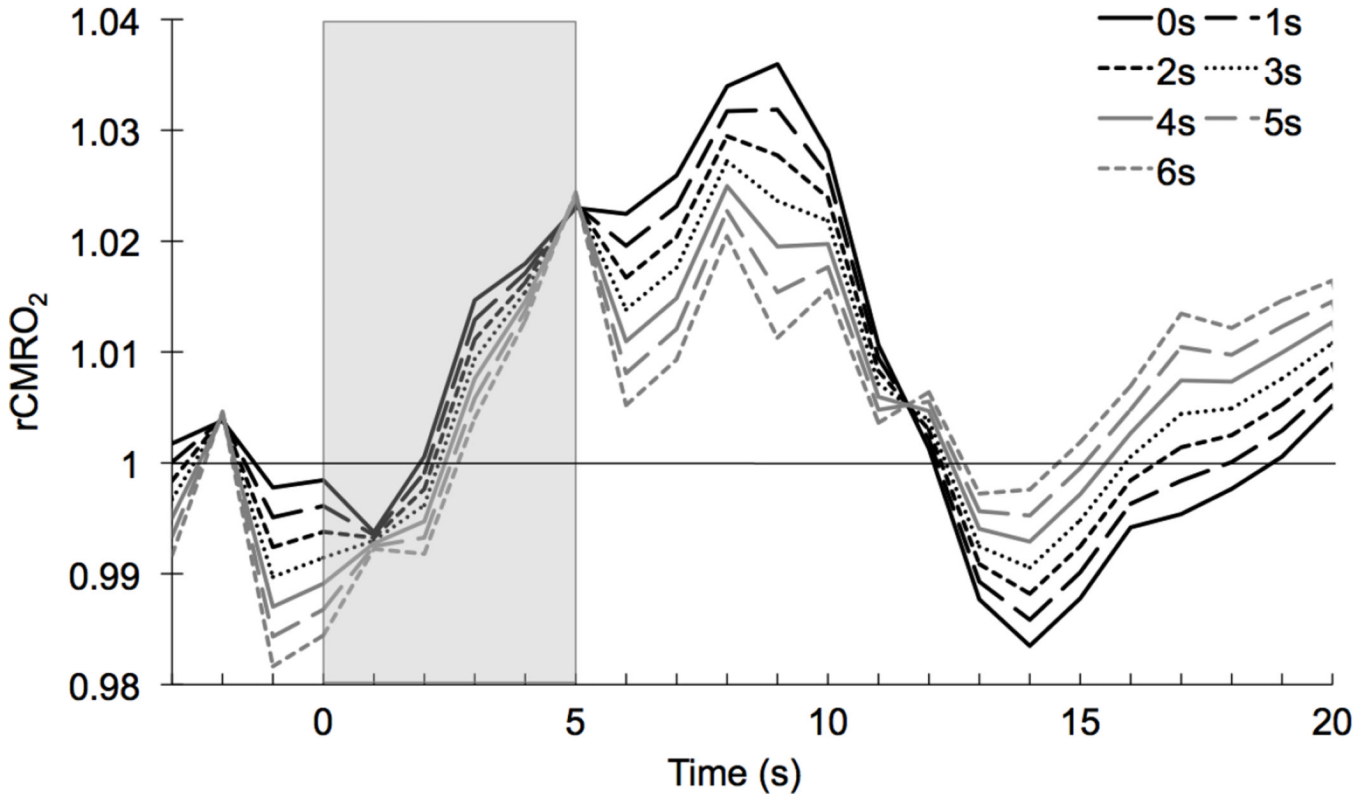


**Fig. 6.**
$rCMRO_2$ calculated using equation (9) for transit times $\tau = 0$ to 6 sec.